

THERMAL SIMULATION MODEL OF AERO-ENGINE BLADE MATERIAL FORGING SIMULATION

by

Huaren DAI^a, Zhe CHEN^b, Wei GUO^a, and Ju WANG^{c*}

^a College of Material Science and Engineering, Jilin University, Changchun, China

^b School of Transportation, Jilin University, Changchun, China

^c College of New Energy and Environment, Jilin University, Changchun, China

Original scientific paper

<https://doi.org/10.2298/TSCI2104169D>

During the high temperature forging process, the thermal parameters such as the temperature field and strain field in the blank have an important influence on the crack damage and micro-structure in the forging. We use the rigid viscoelastic finite element method to carry out the forging process of a heavy aero-engine blade the finite element numerical simulation was carried out to obtain the temperature field, strain field and forging load change law in the forging process with time, and on this basis, combined with the crack damage and repair mechanism and the recrystallization structure evolution law, an optimization was proposed. The forging process plan. That is, the pre-forging is performed on the basis of the tolerance of the final forging dimension under pressure of 4 mm, the pre-forging temperature is 1160 °C, and the final forging temperature is 1120 °C. The actual forging process test verifies the feasibility of the process plan, which is the engineering of this process the application lays the scientific foundation.

Key words: crack damage, micro-structure, aero-engine blade, forging, thermal simulation, numerical simulation

Introduction

The blade is an important part of a heavy-duty gas turbine and plays a key role in energy conversion. Its quality is directly related to the working efficiency and working life of the gas turbine. The shape of the blade is complex, its forging process is poor, and the flow law is difficult to grasp. In the past, due to lack of systematic and accurate theoretical analysis methods, process design mostly adopts trial and error methods, constantly adjusting process parameters and modifying molds, which not only consumes a lot of manpower and material resources, but also prolongs the production cycle [1]. At present, computer numerical simulation has been widely used in blades. In the forging process design, through computer numerical simulation, the forming process can be virtually realized on the computer, and a large amount of information about the amount of deformation field at any time can be obtained, and then the deformation law can be mastered and the forming process can be optimized.

The material used for a heavy-duty gas turbine blade is a new type of martensitic heat-strength stainless steel, which has a low forming limit and a narrow forging range, and the forming conditions have an important influence on the micro-structure of the forging, which in turn affects the performance of the final forging, so it must strictly control the deformation condi-

* Corresponding author, e-mail: wbj1368@163.com

tions and optimize the process parameters. In this paper, the finite element software DEFORM 3-D is used to carry out computer numerical simulation of the forging process of a heavy gas turbine blade. Through comparison and analysis with physical simulation, an optimized process plan is given, and the actual forging the process test verifies the feasibility of the process plan.

Process analysis

The forging of heavy-duty gas turbine blades is a multi-step forging, which is divided into accumulation, forming, flattening, pre-forging and final forging steps. Among them, the accumulation, forming and flattening steps are preformed billet steps. Due to the criticality of metal the deformation is limited, a pre-forging step must be added before the final forging. After the pre-forging is completed, the blank is cooled to room temperature for sanding and sand blowing, and then heated to the final forging temperature for heat preservation [2]. When the temperature inside and outside the blank is uniform, the final forging to obtain the final blade forging. Insufficient pre-forging deformation will cause excessive final forging deformation, resulting in crack damage and structural defects and if the pre-forging deformation is too large, it is likely to produce a large amount of forging cracks and cause insufficient final forging deformation. Therefore, the process design of pre-forging and final forging has an important influence on blade forging.

The pre-forging and final forging of the blade are carried out on a 25 MN crank press. The blade material is a new type of martensitic heat-strength stainless steel. The mechanical properties of the steel are shown in tab. 1. The deformation resistance of this alloy is relatively large, so the forging temperature cannot be too low. If the forging temperature is too high, some brittle phases may be precipitated, thereby reducing the performance of the final forging. The forging temperature is 950-1160 °C.

Table 1. Mechanical properties of blade steel

t [°C]	eb [MPa]	$e_{0.2}$ [MPa]	W [%]	h [%]
20	≥ 1127	≥ 931	≥ 12	≥ 58
500	≥ 925	≥ 770	≥ 12	≥ 60

In the design of the forging process of the blade, the critical deformation of the metal is an important influencing parameter, which determines the amount of metal deformation allowed for each step of the forging. In this paper, the thermoplastic curve of the blade material is measured by the hot compression test. The size is 10 mm × 12 mm. In the test, the sample is heated to the test temperature at a rate of 50 °C per second, kept for 30 seconds, and then compressed at a deformation rate of 10 per second to different degrees of deformation. After the compression is completed, the sample is air-cooled to room temperature. Observe its micro-structure and mechanical properties to determine the critical deformation, W_c , at different deformation temperatures and the influence of different deformation conditions on its mechanical properties [3]. Figure 1 shows the steel thermoplastic curve measured in the test. It can be seen that the blade is used the degree of deformation of steel in one heating does not exceed 60%.

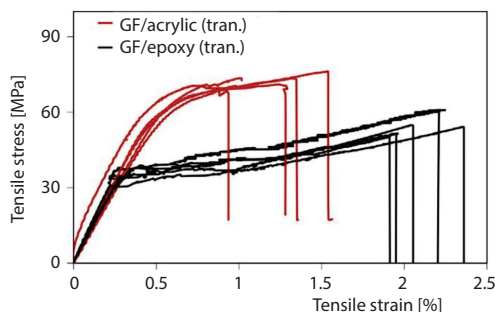


Figure 1. Thermoplastic curve of blade steel

It can be seen that the blade is used the degree of deformation of steel in one heating does not exceed 60%.

Blade-receiver rubbing model

In aero-engines, the main form of rubbing is partial rubbing, that is, rubbing occurs at a fixed position of the casing. Therefore, a local rubbing model of the blade and casing is established, that is, the blade and casing rubbing only at the rubbing point.

Contact basic theory

When the contact objects are all elastomers, the contact pressure on the contact spot is distributed:

$$p = p_0 \left[1 - \left(\frac{r}{a} \right)^2 \right]^{1/2} \quad (1)$$

where p_0 is the maximum normal pressure at the center of the contact spot, a – the radius of the contact spot, and r – the co-ordinate variable within the contact spot. The maximum pressure at the contact center:

$$p_0 = \left(\frac{6FE^*2}{\pi^3 R^2} \right) \quad (2)$$

where F is the normal load, R – the radius of curvature of the contact surface, and E – the elastic modulus of the plane strain problem:

$$\frac{1}{E^*} = \frac{1-\nu_1^2}{E_1} + \frac{1-\nu_2^2}{E_2} \quad (3)$$

$$\frac{1}{R} = \frac{1}{R_1} + \frac{1}{R_2} \quad (4)$$

where E_1, E_2, ν_1, ν_2 is the elastic modulus and Poisson's ratio of the casing and the blade, respectively and R_1, R_2 – the radius of curvature of the contact surface of the casing and the blade, respectively. The radius of the contact spot:

$$a = \left(\frac{3FR}{4E^*} \right)^{1/3} \quad (5)$$

Heat transfer theory and thermal boundary conditions

In order to make the problem easy to handle without losing its meaning, the thermal boundary of the blade-casing rubbing model is simplified:

- ignore the heat loss caused by thermal radiation,
- all frictional heat is converted into temperature,
- the materials are all isotropic,
- the heat transfer coefficient has nothing to do with the spatial position, and
- the change of the density of the structure with temperature is ignored.

According to the aforementioned assumptions, from the basic theory of heat transfer, the internal heat conduction equation of the model in the cylindrical co-ordinate system:

$$\rho c = \frac{\partial T}{\partial t} = K \left(\frac{\partial^2 T}{\partial r^2} + \frac{1}{r} \frac{\partial T}{\partial r} + \frac{1}{r^2} \frac{\partial^2 T}{\partial \theta^2} + \frac{\partial^2 T}{\partial z^2} \right) \dot{Q} \quad (6)$$

where K is the thermal conductivity, T – the temperature, c – the specific heat capacity, ρ – the density, and \dot{Q} – the internal heat source density. The internal heat source density in the blade-casing rubbing model, that is, the frictional heat source on the contact surface:

$$\dot{Q} = \mu p v \quad (7)$$

where v is the linear velocity of the contact point. According to the third type of thermal boundary conditions, the thermal boundary conditions in the unit body:

$$\dot{Q} = -K \nabla T ds = -K \left(\frac{\partial T}{\partial r} + \frac{1}{r} \frac{\partial T}{\partial r} + \frac{\partial T}{\partial z} \right) ds = H(T - T_f) ds \quad (8)$$

where H is the convective heat transfer coefficient and T_f – the ambient temperature.

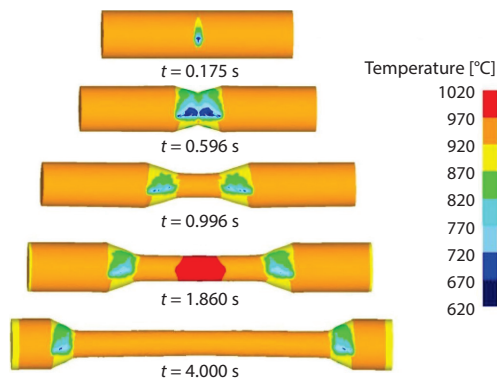


Figure 2. The mesh deformation of the blank during the numerical simulation

The material used for the blades of the heavy-duty gas turbine is a new type of martensitic heat-strength stainless steel, and its high temperature mechanical properties and thermal physical properties are measured through experiments. The flow stress model of rigid viscoelastic materials is $\bar{\sigma} = \bar{\sigma}(\bar{X}, \bar{X}, \bar{T})$, that is, the flow stress and equivalent plastic strain of the material \bar{X} . The strain rate \bar{X} is related to the temperature T . In the calculation, the piecewise linearization method is adopted, and the input is taken according to the high temperature mechanical properties measured in the test. The initial temperature of the pre-forged blank is 1160 °C, and the die should be preheated according to the process specification, the preheating temperature is 300 °C. In the multi-step simulation process, the blank completed by the previous step is used as the initial blank of the next step, but the initial conditions of the blank must be reset. The friction between the blank and the mold using shear friction model:

$$f_s = mk \quad (9)$$

where f_s is the friction force, k – the shear yield strength, m – the friction factor, and its size is related to the interface contact state, which is taken as 0.3. The interface heat transfer coefficient between the blank and the mold during the simulation is taken as 11 kW/m²°C.

Numerical simulation results and analysis

In order to clearly grasp the overall deformation of the blade from the pre-formed blank to the final blade forging, the pre-forging step before the final forging is not considered for the time being, and the pre-formed blank is directly placed in the final forging die for one-

Establishment of finite element model

The profile of the blade mold is very complicated. Therefore, the accuracy of the forging die geometry directly determines the reliability of the numerical simulation results. First, the UG geometric modelling software is used to accurately shape the mold and blank, and then define and calculate in DEFORM 3-D. Since the forging of the blade is a high temperature and large deformation process, the elastic deformation of the blank is negligible, the rigid viscoelastic material model is used, and the mold is set as a rigid body [4]. Figure 2 shows the grid deformation diagram of the blank during the numerical simulation.

step forging. Through the analysis of the deformation process based on the equivalent strain and the distribution of the temperature field, we obtained the overall deformation law of the blade forming, and then optimized the forging process on this basis.

Equivalent strain analysis

During the final forging, with the movement of the upper die, the blank metal flows laterally to both sides of the inlet and outlet edges, and flows longitudinally to the tip of the blade to fill the entire cavity, and the typical cross-section of the blade body is taken to analyze its deformation law. The equivalent strain distribution contour map in the AA section of the blade body after the final forging is given. It can be seen that the blade body has undergone a large plastic deformation after the final forging is completed, and the final forging is completed in most areas of the AA section. The equivalent strain is 1.33-1.61. Compared with the thermoplastic curve of the steel in fig. 1, it can be seen that the final forging deformation has far exceeded the plastic forming limit of the steel, which is very likely to cause cracks. One of the important characteristics of high temperature plastic deformation is the damage of the crack during the deformation process and the crack repair due to recrystallization and diffusion. On the one hand, the micro-cracks formed at the inclusions under the deformation conditions may expand and grow, on the other hand, the metal structure recrystallizes the role of the crack tip is to passivate the crack tip and inhibit its development [5]. At the same time, under the action of external force, the crack surface begins to contact, and the contact part is welded through recrystallization and diffusion, and the formed crack may be repaired. In order to eliminate forging for the inclusion cracks generated in the process, the forging process can reserve the amount of deformation and use the final forging process to repair the defects, that is, the pre-forging process eliminates porosity defects, and the final forging process controls the inclusion cracks. Another way to control the final forging fire the purpose is to ensure that the grain size in the forging is not coarse and to avoid the occurrence of mixed crystals, fig. 3.

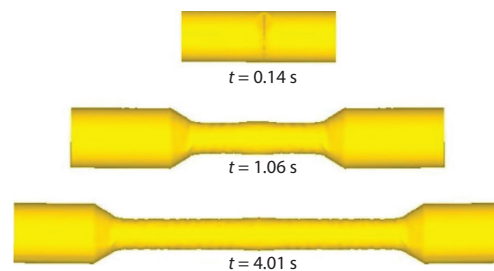


Figure 3. Equivalent strain distribution of AA section after final forging

Temperature field analysis

Temperature, as one of the basic parameters of deformation, has a direct impact on the grain size, grain uniformity, forming process and die life of the forging. Since the material used in the gas turbine blade is extremely sensitive to the forging temperature, the blank must be strictly controlled during the blade forging, fig. 4 shows the contour map of the temperature distribution in the AA section of the blade body after the final forging. It can be seen from the figure that the highest temperature area appears in the body and the ends of the leaf, while the lowest temperature area appears in the mold contact area. Due to the contact heat transfer with the upper and lower molds, the surface temperature of the blade body has dropped, but it is still higher than the material's stop forging temperature (950 °C). The body and the body of the blade are less cooled by the mold. As the deformation process progresses, the heat generated by the plastic work also has a certain compensation effect on the temperature of the core, so the maximum temperature of the body and the body of the leaf reaches 1170 °C, and the temperature at both ends of the leaf body is as high as 1190 °C due to the violent friction. When the

blade is formed, the surface temperature is low, and when the degree of deformation is small, it is easy to be in a critical deformation state, and coarse surface crystals appear, which makes the

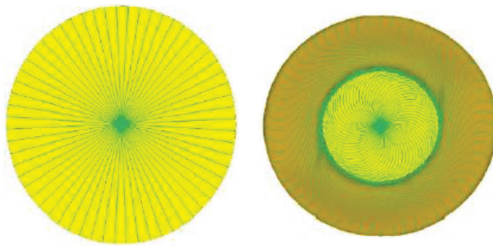


Figure 4. Temperature field distribution of AA section after final forging

surface and core of the blade uneven, and the overall strength of the forging decreases [6]. Therefore, the final forging deformation must be controlled. Temperature to reduce the temperature difference. For the martensitic heat-strength stainless steel used in the blade, too high temperature will easily cause the precipitation of some brittle phases, which will reduce the strength and toughness of the blade, so the final forging temperature should be appropriately reduced.

Optimization of forging process

Through the analysis of the aforementioned numerical simulation results, it can be seen that the deformation of the blade body is too large when the final forging is completed, exceeding the critical deformation of the blade material, and due to the large temperature difference between the inside and outside of the blade, the mixed crystal phenomenon may occur. A pre-forging step is added before the final forging. Through a large number of simulation calculations, this paper finally gives an optimized forging process plan, that is, the pre-forging is performed with a 4 mm under pressure based on the tolerance of the final forging size. If the under pressure is greater than 4 mm, the final forging deformation is too large, which exceeds the critical deformation of the material and if the under pressure is less than 4 mm, the pre-forging deformation is too large, and the subsequent final forging deformation is insufficient, so that it cannot be fully repaired defects and recrystallization.

From the aforementioned temperature field analysis results, it can be seen that due to the influence of the heat generated by plastic work and the heat generated by friction, the surface temperature of the blade body during the forging process is small, and the temperature of the body and the inlet and exhaust edges of the blade body and both ends is too high [7]. This leads to the precipitation of some brittle phases, which affects the performance of the blade forgings, so the final forging temperature should be appropriately reduced. The deformation resistance of the blade material is extremely sensitive to temperature, and the temperature decreases, and the deformation resistance of the material increases sharply, which leads to a sharp increase in the forging load, so the final forging temperature should ensure that the forging load is within the rated load range of the equipment. Through the comparison and analysis of the results of physical simulation and numerical simulation, the final forging temperature is determined to be 1120 °C.

Analysis of numerical simulation results of optimized process plan

Figure 5 shows the contour map of the equivalent strain distribution in the AA section of the blade body when the pre-forging and final forging are completed under the optimized process plan (that is, the pre-forging is performed with a 4 mm under pressure based on the tolerance of the final forging size). It can be seen that the equivalent strain in the AA section of the blade body after the pre-forging is between 0.422 and 1.0, and the equivalent strain in the AA section of the blade body after the final forging is between 0.3 and 0.6. Compared with the original forging process plan, after process optimization, the final forging accumulated strain

is greatly reduced, which is lower than the critical deformation of the material, and at the same time, it reaches a certain degree of deformation, so that defect damage and full recrystallization can be fully repaired, and the quality of the final blade forging is guaranteed [8]. Although the equivalent strain after completion is slightly higher, since the blank has to be reheated and kept for final forging after the pre-forging is completed, even if a small amount of micro-cracks are generated in the pre-forging, the subsequent final forging can also repair it, so it does not affect the performance of the final forging.

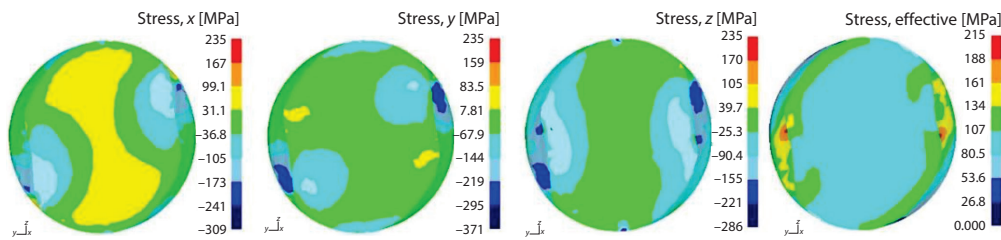


Figure 5. Equivalent strain distribution of AA section of the blade body after pre-forging and final forging under the optimized process plan

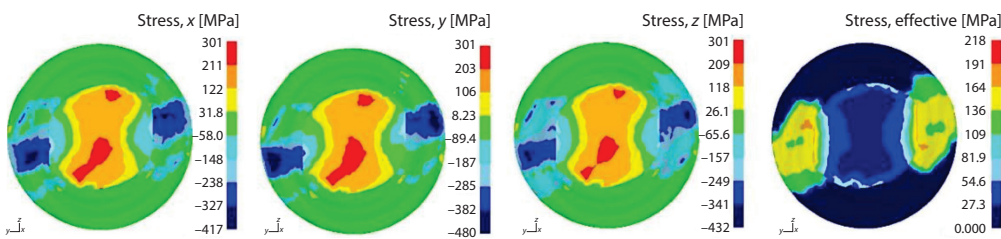


Figure 6. Temperature field distribution of AA section after final forging under optimized process plan

Figure 6 shows the contour map of the temperature field distribution in the AA section of the blade body when the final forging is completed under the optimized process plan. It can be seen that due to the small deformation of the final forging, the time is shorter, and the blank is in the blank when the final forging is completed. The temperature change is not large, most areas are still 1120 °C, which reduces the temperature difference, thus avoiding the occurrence of coarse grains and mixed crystals. Because the final forging temperature is reduced to 1120 °C, the amount of plastic deformation is small, and there is no causes the temperature to rise, thereby reducing the precipitation of brittle phases, and ensuring the quality of the final forging [9]. Due to the large deformation, the friction is severe, and the temperature rises slightly. However, the flash part needs to be removed after forging. The performance of forgings has no effect.

Figure 7 is the curve of the forging load change with time under the optimized process plan. It can be seen that due to the small flash during pre-forging, the deformation of the blank is similar to free upsetting, the load is small, and the flash during final forging is larger. The defor-

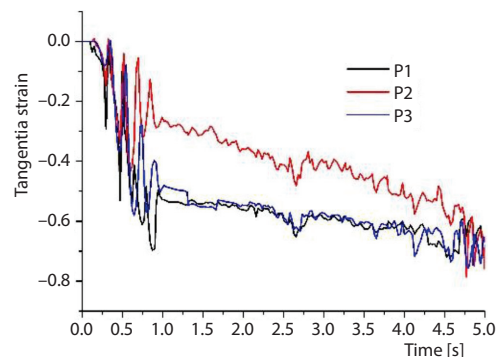


Figure 7. Load change curve under optimized process plan

mation resistance increases, and due to the lower final forging temperature, the metal deformation resistance is higher, and the load increases sharply [10]. The maximum value reaches 23 MN. The rated load of the crank press used for the final forging is 25 MN, so the forging load under the optimized process plan is still fulfil requirements.



Figure 8. Forging process test with optimized process plan

The inspection of the micro-structure and mechanical properties of the final forging showed that its performance met the process requirements, thereby verifying the feasibility of the optimized process plan and providing a scientific basis for the engineering application of the process plan.

Test verification of optimized process plan

In order to verify the feasibility of the optimized process plan, a forging process test was carried out on site, and the process plan was verified with the actual produced blade forgings. Figure 8 shows the final forging die lower die and preformed blank diagram in the forging process test. The inspection of the micro-structure and mechanical properties of the final forging showed that its performance met

Conclusion

The paper uses the rigid viscoelastic finite element method to numerically simulate and analyze the forging process of a heavy gas turbine blade. The temperature field, strain field distribution and load change curve in the forging during the deformation process are obtained, which provides for the optimization design of the forging process. Under the conditions of the final forging process that does not consider the pre-forging step, the strain value in the forging is higher, which exceeds the critical deformation of the blade material, which is very likely to cause the generation of forging defects. Due to the heat and heat generated by the plastic work due to friction and heat generation, the temperature of the body and the body of the leaf is higher, and the temperature difference between the surface and the core is large, which may cause the occurrence of coarse grains and mixed crystals, which may cause the performance of the forging to decrease. In the comparison and analysis of the previous numerical simulation results and physical simulation tests on the basis of, combined with the forging crack damage and repair mechanism and the recrystallization structure evolution law, this article gives an optimized forging process plan, that is, under pressure 4 mm for pre-forging based on the tolerance of the final forging size, and the pre-forging temperature is 1160 °C, the final forging temperature drops to 1120 °C. Numerical simulation results show that the temperature field, strain field and forging load in the forging under the process conditions meet the process requirements. The actual forging process test verifies the feasibility of the process plan.

References

- [1] Wu, S., Construction of Visual 3-D Fabric Reinforced Composite Thermal Performance Prediction System, *Thermal Science*, 23 (2019), 5, pp. 2857-2865
- [2] Xiuquan, H., Dingxi, W., Efficient Determination of Turbomachinery Blade Aero-Damping cCurves for Flutter Assessment Via Trigonometric Interpolation, *Journal of Thermal Science*, 29 (2020), 3, pp. 763-771
- [3] Li, J. W., *et al.*, Casting Design Optimization Using Numerical Simulation of Precision Forging Die for Large Titanium Alloy Integral Bulkhead, *International Journal of Metalcasting*, 13 (2019), 4, pp. 830-844
- [4] Cai, J. M., *et al.*, Research Progress in Manufacturing Technology of 600 °C High Temperature Titanium Alloy Dual Property Blisk Forging, *Cailiao Gongcheng/Journal of Materials Engineering*, 46 (2018), 5, pp. 36-43

- [5] Hong, J., *et al.*, Dynamic Response of the Aero-Engine Flexible Rotor System under the Blade-off, *Hangkong Dongli Xuebao/Journal of Aerospace Power*, 33 (2018), 2, pp. 257-264
- [6] Tsutsumi, S., *et al.*, Improvement of Aero-Vibro Acoustic Simulation Technique for Prediction of Acoustic Loading at Lift-off, *The Journal of the Acoustical Society of America*, 44 (2018), 3, pp. 1672-1672
- [7] Weng, H., *et al.*, Electrical Insulation Improvements of Ceramic Coating for High Temperature Sensors Embedded on Aeroengine Turbine Blade, *Ceramics International*, 46 (2020), 3, pp. 3600-3605
- [8] Dong, Y., *et al.*, An Improved Canny Operator Used for Aero-Engine's Blade Welding and Repairing, *Hanjie Xuebao/Transactions of the China Welding Institution*, 39 (2018), 1, pp. 37-40
- [9] Wu, S., Study and Evaluation of Clustering Algorithm for Solubility and Thermodynamic Data of Glycerol Derivatives, *Thermal Science*, 23 (2019), 5, pp. 2867-2875
- [10] Guan, P., *et al.*, Structural Strength Simulation of Film Cooling Vane after Heat Shock by Thermal/Flow/Structure Coupling, *Hangkong Dongli Xuebao/Journal of Aerospace Power*, 33 (2018), 8, pp. 1811-1820